A Thesis for the Degree of Master of Science

In vitro antimicrobial activity and mode of action of erythorbyl laurate, a novel antimicrobial agent, against *Staphylococcus aureus*

*Staphylococcus aureus*에 대한 erythorbyl laurate의 항균성 메커니즘 규명

August, 2014

Jo, Su Kyung

Department of Agricultural Biotechnology

Seoul National University

In vitro antimicrobial activity and mode of action of erythorbyl laurate, a novel antimicrobial agent, against *Staphylococcus aureus*

지도교수 장 판 식

이 논문을 석사학위 논문으로 제출함

2014년 8월

서울대학교 대학원 농생명공학부

조 수 경

조수경의 석사 학위 논문을 인준함

위 원 장 강 동 현 (인)

부위원장 장 판 식 (인)

위 원 최 영 진 (인)

Abstract

Based on the results of susceptibility screening (spot-on-lawn assay) and bactericidal activity, it was found that erythorbyl laurate (6-*O*-lauroyl-erythorbic acid) had effect on gram positive bacteria. For evaluating antimicrobial activity of erythorbyl laurate against gram positive bacteria, minimum inhibitory concentration (MIC) and minimum bactericidal concentration (MBC) were assessed by broth micro-dilution method. With sub-MICs of erythorbyl laurate, gram positive bacteria showed increased lag time ($\Delta\lambda$) and decreased maximum specific growth rate (μ_{max}) compared to control without erythorbyl laurate treatment. *S. aureus* showed maximum crystal violet uptakes at 1.2-1.6 mM of erythorbyl laurate. Samples treated with positive control, nisin (40 mg/mL), of which mechanism was induction of pore formation on membranes increased permeability similar to maximum crystal violet uptake levels of each bacteria samples treated with erythorbyl laurate. Exposure of *S. aureus* to erythorbyl laurate at various concentrations showed altered cytoplasmic membrane rupture, and these were assessed by using the Live/Dead BacLight viability kit. Relative live percentage of *Staphylococcus aureus* reached 0% below 1.6 mM erythorbyl laurate.

Morphological analysis was performed by EF-TEM, and inhibitory and bactericidal concentrations indicated that erythorbyl laurate addition caused dissolution of the cytoplasmic space, significant roughing of the membrane, and cytoplasmic convolution. In combination with other antimicrobial agents, nisin, kanamycin, and erythromycin showed great synergistic effect with erythorbyl laurate with 0.281, 0.256, and 0.266 of fractional inhibitory concentration (FIC) index, respectively. Transcriptional changes of *S. aureus* treated with erythorbyl laurate showed significantly different patterns compared to those of sample without erythorbyl laurate treatment, including genes related with amino acid synthesis, cell envelope, protein function, cellular processes, regulatory function, and signal transduction.

Keywords: erythorbyl laurate; multi-functional food additives; antimicrobial agent; mechanism; RNA sequencing; transcriptome

Student Number: 2012-23391

Contents

List of tables

List of figures

1. Introduction

Erythorbic acid, a stereoisomer of L-ascorbic acid, has been extensively used as an antioxidant, but cannot be applied to lipid-based foods due to poor lipophilicity. For these reasons, lipase-catalyzed esterification between lauric acid and erythorbic acid in the previous work was performed to produce erythorbyl laurate (EL), a novel multi-functional emulsifier with antioxidative and antimicrobial activity (Park, Lee, Sung, Lee, & Chang, 2011).

It has been reported that lauric acid and its derivatives possess growth-inhibitory effects against a wide range of microorganisms and the antimicrobial activity was markedly influenced according to the non-fatty acid moiety (Lieberman, Enig, & Preuss, 2006; Nobmann, Bourke, Dunne, & Henehan, 2010; Sands, Landin, Auperin, & Reinhardt, 1979). As had been anticipated from the previous reports of lauric acid, erythorbyl laurate showed growth-inhibitory effect on a range of pathogens. Particularly, gram-positive pathogens such as *Listeria monocytogenes*, *Bacillus cereus,* and *Staphylococcus aureus* were very susceptible to erythorbyl laurate, while it had no significant effect on gram-negative bacteria.

Understanding how pathogens respond to a novel antimicrobial agent,

and how this works compared with other currently available antimicrobial agents are crucial for optimizing treatment conditions of certain antimicrobial agent (Friedman, Alder, & Silverman, 2006; Muthaiyan, Silverman, Jayaswal, & Wilkinson, 2008; Pietiainen, Francois, Hyyrylainen, Tangomo, Sass, Sahl, et al., 2009). For the study of antibacterial mechanism of erythorbyl laurate, *Staphylococcus aureus* which is one of severe human pathogens and common cause of food poisoning was subject for the experiments.

The objective of this study was to verify antimicrobial activity and mechanism of erythorbyl laurate against food-borne pathogens, which could be used as a multifunctional antimicrobial agent. First of all, the effectiveness of erythorbyl laurate was validated by determination of effective concentration and physiological experimentation. To further understand the mechanism, transcriptome analysis of changes in gene expression of erythorbyl laurate-treated *Staphylococcus aureus* Newman was carried out by next generation sequencing. It was found out whether there are strong erythorbyl laurate-specific responses or general response triggered by erythorbyl laurate exposition. It contributed to explore the mode of action of erythorbyl laurate and to apply erythorbyl laurate as multi-functional food additives and antimicrobial agents in various industries properly.

2. Materials and methods

2-1. Cell culture

Ten gram positive strains were *Listeria monocytogenes* ATCC 7644, ATCC 19114, ATCC 19115, *Bacillus cereus* ATCC 10876, ATCC 13061, *Staphylococcus aureus* ATCC 12692, ATCC 27213, ATCC 29213, ATCC 49444 and Newman. Seven gram negative strains were *Escherichia coli* ATCC 35150, ATCC 43890, *Salmonella* Typhimurium ATCC 19585, ATCC 19586, ATCC 43970, *Pseudomonas aeruginosa* ATCC 10145 and ATCC 15692. All the microorganisms were cultured overnight at 37°C in tryptic soy broth.

2-2. Zone of growth inhibition assay (Spot-on-lawn)

Antimicrobial susceptibility of erythorbyl laurate was assessed by a zone of growth inhibition assay. Tryptic soy agar plate was overlaid with 5 mL of tryptic soy 0.4% soft agar (w/v %) that was inoculated with 10^8 CFU/mL of exponentially growing bacterial suspension (Jin, Li, Wang, Wang, Huang, Li, et al., 2012; Pan, Cheung, & Link, 2010; Salvucci, Saavedra, & Sesma, 2007). All bacteria described above was subjected to this assay. After solidification, 5 μL of erythorbyl laurate sample was spotted

onto the soft agar overlay. The plates were incubated at 37 °C overnight and then analyzed for growth inhibition zones.

2-3. Bactericidal and bacteriostatic activity

2-3-1. Bactericidal activity of erythorbyl laurate

Escherichia coli ATCC 35150, *Salmonella* Typhimurium ATCC 19586, *Listeria monocytogenes* ATCC 19114, and *Staphylococcus aureus* ATCC 27213 were tested for verifying bactericidal effect of erythorbyl laurate. Erythorbyl laurate, erythorbic acid and lauric acid were each dissolved in 1% ethanol in tryptic soy broth, and each of bacterial suspension was added adjusting to 10^6 CFU/mL. After incubation at 37°C for 30 minutes, 0.1 mL of each of the 10-fold serial dilutions were spread on tryptic soy agar plates. Then, colony counting was performed after incubation at 37°C for 24 h.

2-3-2. Minimum inhibitory concentration (MIC) and minimum bactericidal concentration (MBC)

Listeria monocytogenes ATCC 7644, ATCC 19115, *Bacillus cereus* ATCC 10876, ATCC 13061, *Staphylococcus aureus* ATCC 12692, ATCC

29213, and ATCC 49444 were tested for determination of effective concentration of erythorbyl laurate. MIC and MBC, which are standard criteria for evaluation of antimicrobial effect, were determined by broth micro-dilution assay. Briefly, serial dilutions of each desired concentration of erythorbyl laurate were prepared in sterile tryptic soy broth to final volume of 100 μL in 96-well microplate (Corning). Then, each well was inoculated with 100 μL of test organisms in tryptic soy broth to final concentration of 5×10^5 CFU/mL (Bechert, Steinrucke, & Guggenbichler, 2000; Magalhaes & Nitschke, 2013; Nobmann, Bourke, Dunne, & Henehan, 2010; Wiegand, Hilpert, & Hancock, 2008). The MIC was taken as the lowest concentration of test compound at which bacterial growth was inhibited after 12 h of incubation at 37°C. Then, the MBCs of erythorbyl laurate against each isolate was reported as the lowest concentration producing a 99.9% reduction in bacterial viable count in the sub-cultured well contents. 10-fold serially diluted sub-cultured well contents was spread on to tryptic soy agar plates and counting the colonies (Pridmore, Burch, & Lees, 2011).

2-3-3. Increase in lag time (Δλ) and maximum specific growth rate (μ_{max})

Increase in lag time (Δλ) was calculated using data from absorbance-based broth micro-dilution assays using SoftMax Pro Version 5.3 software

(Molecular Devices). The $\Delta\lambda$ was defined as the time required for the bacteria growth with erythorbyl laurate to record an increase in OD_{600} value compared to that of the culture without erythorbyl laurate (Gutierrez, Barry-Ryan, & Bourke, 2008; Nobmann, Bourke, Dunne, & Henehan, 2010). Maximum specific growth rate (μ_{max}) was auto-calculated by SoftMax Pro.

2-4. Crystal violet assay

The bacterial strains were grown in tryptic soy broth at 37°C for overnight, harvested and washed with phosphate buffer saline (PBS) at pH 7.4. The bacterial cells were treated in the range of 0.4–3.2 mM of erythorbyl laurate at 37°C (Bharali, Saikia, Ray, & Konwar, 2013; Devi, Nisha, Sakthivel, & Pandian, 2010). Ampicillin (50 μg/mL) and nisin (40 mg/mL) were used as positive controls. Both erythorbyl laurate-treated and non-treated samples were resuspended in crystal violet solution (30 μg/ml) prepared in PBS and incubated at 37 °C for 30 min. The percentage of crystal violet dye uptake by the samples was calculated using the formula:

$$\text{Crystal violet uptake (\%)} = \frac{\text{OD}_{590} \text{ value of the sample}}{\text{OD}_{590} \text{ value of the crystal violet solution}} \times 100$$

2-5. Assessment of cell rupture with fluorescence

2-5-1. Fluorescence intensity of SYTO 9 and propidium iodide

The Live/Dead BacLight viability kit (Molecular Probes, Inc.) was used for assessment of cell rupture level according to the manufacturer's instructions. In this assay, the SYTO 9 and propidium iodide stains compete for binding to the bacterial nucleic acid. SYTO 9 labels cells with both damaged and intact membranes, whereas propidium iodide penetrates only cells with damaged membranes. A culture of *S. aureus* ATCC 29213 as a model organism was grown to late log phase in tryptic soy broth. The bacterial culture was concentrated by centrifugation at 10000×g for 10 min. The supernatant was removed and the pellet was washed once with PBS (pH 7.4). Bacterial suspension was added to sterile PBS for live bacteria estimation and to 70% isopropyl alcohol for dead bacteria estimation. Both Live and dead cells were adjusted to 2×10^7 CFU/mL. Different proportions of the live and dead cells were mixed to obtain cell suspensions containing five different ratios (100:0, 75:25, 50:50, 25:75 and 0:100 in %), of live and dead cells for a data set to provide a standard curve. Standard curve was plotted on the Ratio $_{G/R}$ versus percentage of live cells.

Overnight grown *S. aureus* was washed and resuspended in PBS. Bacterial suspension and control sample adjusted to 2×10^7 CFU/mL were

treated with erythorbyl laurate and incubated at 37 °C for 30 min. At the end of the incubation period, the suspensions were centrifuged at 10000×g for 10 min, washed once in PBS again. A volume of 100 µL of each bacterial suspension was added into separate wells of a black 96-well microplate with clear bottom (Nunc). Preparing the stain solution and measuring fluorescent intensity were performed according to the manufacturer's instructions. Briefly, the stain solution was prepared by mixing 3.34 mM SYTO 9 (green) and 20 mM propidium iodide (red) in equal proportion. To each well, 100 µL of stain solution was added, and the plate was incubated in the dark for 15 min at room temperature. At the end of the incubation period, with the excitation wavelength centered at 485 nm, the emission fluorescence intensity was measured for SYTO 9 (green, G) at 530 nm and propidium iodide (red, R) at 630 nm.

$$\text{Ratio}_{\text{G/R}} = \frac{\text{Green emission fluorescence intensity}}{\text{Red emission fluorescence intensity}}$$

2-5-2. Fluorescent microscopy

Overnight grown *S. aureus* was washed and resuspended in 0.85% NaCl solution. As described above, bacterial suspension and control sample adjusted to 1×10^5 CFU/mL were treated with erythorbyl laurate and

incubated at 37 °C for 30 min. At the end of the incubation period, 3 μL of the dye mixture added for each mL of bacterial suspension. After incubation in the dark at room temperature, 5 μL of stained bacterial suspension was trapped between a slide and coverslip and observed in fluorescence microscope (Carl Zeiss, DE/Axio imager A1) equipped with fluorescence filters for SYTO 9 (Carl Zeiss, filter set 38 HE) and propidium iodide (Carl Zeiss, filter set 43 HE).

2-6. Energy filtered transmission electron microscopy (EF-TEM)

To prepare specimen for energy filtered transmission electron microscopy (EF-TEM), the overnight culture of *S. aureus* ATCC 29213 were treated with erythorbyl laurate at MIC and 4×MIC for 12 h at 37°C. The untreated (control) and erythorbyl laurate-treated cells were harvested by centrifuge (13,000×g, 5 min). The pellets were fixed (primary fixation) with Modified Karnovsky's fixative 2% paraformaldehyde and 2% glutaraldehyde in 0.05 mM sodium cacodylate buffer (pH 7.2) at 4°C for two to four hours, and were washed with 0.05 mM sodium cacodylate buffer at 4°C for 10 min. After primary fixation, samples were fixed (post-fixation) with 1% osmium tetroxide in 0.05 mM sodium cacodylate buffer at 4°C for two hours, and were shortly washed using distilled water at room temperature. After

transition with 100% propylene oxide, samples were dehydrated at room temperature for 10 min with increasing concentration of ethanol (30, 50, 70, 80, 90, 100%) and were infiltrated with Spurr's resin. Then, samples were dried for 24 hours. Specimen was investigated using EF-TEM (LIBRA 120, Carl Zeiss) under standard operating condition (Kim & Chung, 2011).

2-7. Synergistic effect with antibiotics and food additives

The synergistic effects between erythorbyl laurate and antimicrobials were assessed by the checkerboard test (Gutierrez, Barry-Ryan, & Bourke, 2008; Magalhaes & Nitschke, 2013). The checkerboard test was elaborated using a 96-well microplate with serial dilutions of erythorbyl laurate and other antimicrobial samples. The diluted samples of erythorbyl laurate were prepared in the vertical rows and other antimicrobial samples in the horizontal columns, and serial dilutions of two different antimicrobial agents were mixed in tryptic soy broth. The micro-broth dilution technique was performed as described above in MIC determination. After 12 h of incubation at 37 °C, the FIC index was calculated employing MIC of the antimicrobial compounds alone and the respective MIC when the compounds were combined. The classification of the antimicrobial interaction was made using the following parameters: when the FIC index is ≤ 0.5, the interaction

is synergistic, when the FIC index is > 0.5 and ≤ 4, the interaction is indifferent, and the FIC index > 4 defines the antagonistic interaction. The FIC index (∑FIC) was determined using the following equation:

$$\sum \mathrm{FIC} = \frac{\text{MIC of EL in combination}}{\text{MIC of EL}} + \frac{\text{MIC of antimicrobial agent in combination}}{\text{MIC of antimicrobial agent}}$$

$$= \mathrm{FIC}_{\mathrm{EL}} + \mathrm{FIC}_{\text{Antimicrobial agent}}$$

2-8. Transcriptional analysis by RNA-Seq

The effects of erythorbyl laurate on gene expression of *S. aureus* Newman were studied by RNA-Seq. The two total RNA samples were pooled for transcriptome analysis to obtain the gene expression information.

2-8-1. Extraction and purification of RNA from *S. aureus*

Overnight-grown *S. aureus* Newman was inoculated in tryptic soy broth (40 mL) in Erlenmeyer flask (100 mL) at 37°C with shaking at 220 rpm until the optical density reached 0.8. Samples were taken for RNA extraction and treated with sublethal concentration of erythorbyl laurate (0.1 mM) for 15 min. Control cultures without addition of erythorbyl laurate were also incubated in the same condition for 15 min. After incubation, total RNA extraction using Easy-RED BYF total RNA extraction kit (INtRON

Biotechnology, Inc.) was used to extract the total RNA from the two samples. DNase digestion and RNA cleanup were performed with RNase-Free DNase set (Qiagen) and RNeasy MinElute cleanup kit (Qiagen) according to the manufacturer's instructions, respectively.

2-8-2. cDNA libraray construction

The mRNA in total RNA was converted into a library of template molecules suitable for subsequent cluster generation using the reagents provided in the Illumina ® TruSeq™ RNA Sample Preparation Kit. The first step in the workflow involved removing the rRNA in the total RNA using Ribo-Zero rRNA Removal kit (Epicentre). Following this step, the remaining mRNA was fragmented into small pieces using divalent cations under elevated temperature. The cleaved RNA fragments were copied into first strand cDNA using reverse transcriptase and random primers followed by second strand cDNA synthesis using DNA polymerase I and RNase H. These cDNA fragments went through an end repair process, the addition of a single 'A' base, and ligation of the adapters. The products were purified and enriched with PCR to create the final cDNA library.

2-8-3. RNA-Seq data analysis

RNA-Seq reads were mapped by using TopHat (http://tophat.cbcb.umd.edu/index.html). It aligns RNA-Seq reads to mammalian-sized genomes using the ultra high-throughput short read aligner Bowtie, and then analyzes the mapping results to identify splice junctions between exons. Assembling transcripts and estimating their abundances performed by using Cufflinks (http://cufflinks.cbcb.umd.edu/index.html), and it analyzed differential expression and regulation in RNA-Seq samples. It accepts aligned RNA-Seq reads and assembles the alignments into a parsimonious set of transcripts. Cufflinks then estimates the relative abundances of these transcripts based on how many reads support each one, taking into account biases in library preparation protocols. Then, SAM (Sequence Alignment/Map, http://samtools.sourceforge.net/cns0.shtml) was used to manipulating alignment in the SAM format, a flexible generic format for storing nucleotide sequence alignment. To utilize up-to-date information to functionally annotate genetic variants detected from diverse genomes, list of variants with chromosome, start position, end position, reference nucleotide and observed nucleotides was analyzed with ANNOVAR (http://www.openbioinformatics.org/annovar/). For gene fusion discovery, DeFuse software (http://sourceforge.net/apps/mediawiki/defuse/index.php?title=Main_Page) was used.

2-9. Quantitative real-time RT-PCR (qRT-PCR)

cDNA was synthesized by using QuantiTect reverse transcription kit (Qiagen). The qRT-PCR was performed by using specific primer pairs and iQ^{TM} SYBR Green supermix (Biorad). Primers were designed with the Primer-BLAST (NCBI) and purchased from Macrogen. The amplification and detection of PCR products were performed with CFX Connect^{TM} Real-Time System (Biorad). The thermal cycling conditions: After polymerase activation and DNA denaturation at 95^{o}C, amplification step for 40 cycles repetition were performed with denaturation step at 95^{o}C, annealing and extension step at 55^{o}C.

These cDNA values were normalized with the value of 16s rRNA, which was constant in different conditions (data not shown).

3. Results and discussion

3-1. Susceptibility screening

In spot-on-lawn assay, erythorbyl laurate showed antimicrobial activity to tested gram positive bacteria. The erythorbyl laurate was active against *Staphylococcus aureus*, *Listeria monocytogenes*, and *Bacillus cereus* at concentrations of at least 1 mM, whereas *Escherichia coli*, *Salmonella* Typhimurium, and *Pseudomonas aeruginosa* were resistant to erythobyl laurate. Figure 1 shows results of gram positive bacteria partially.

In all tested gram positive bacteria, inhibition activity of erythorbyl laurate was proportionate to concentration in the range from 1 to 4 mM, and showed more apparent clear zone and better antimicrobial effect than that of lauric acid from which erythorbyl laurate were made. These results demonstrated that antimicrobial activity of erythorbyl laurate was output from the synergism resulting from esterification between erythorbic acid and lauric acid. The similar or slightly better antibacterial activity of the erythorbyl laurate was comparable to the 2-fold serial diluted standard antimicrobial agent, penicillin.

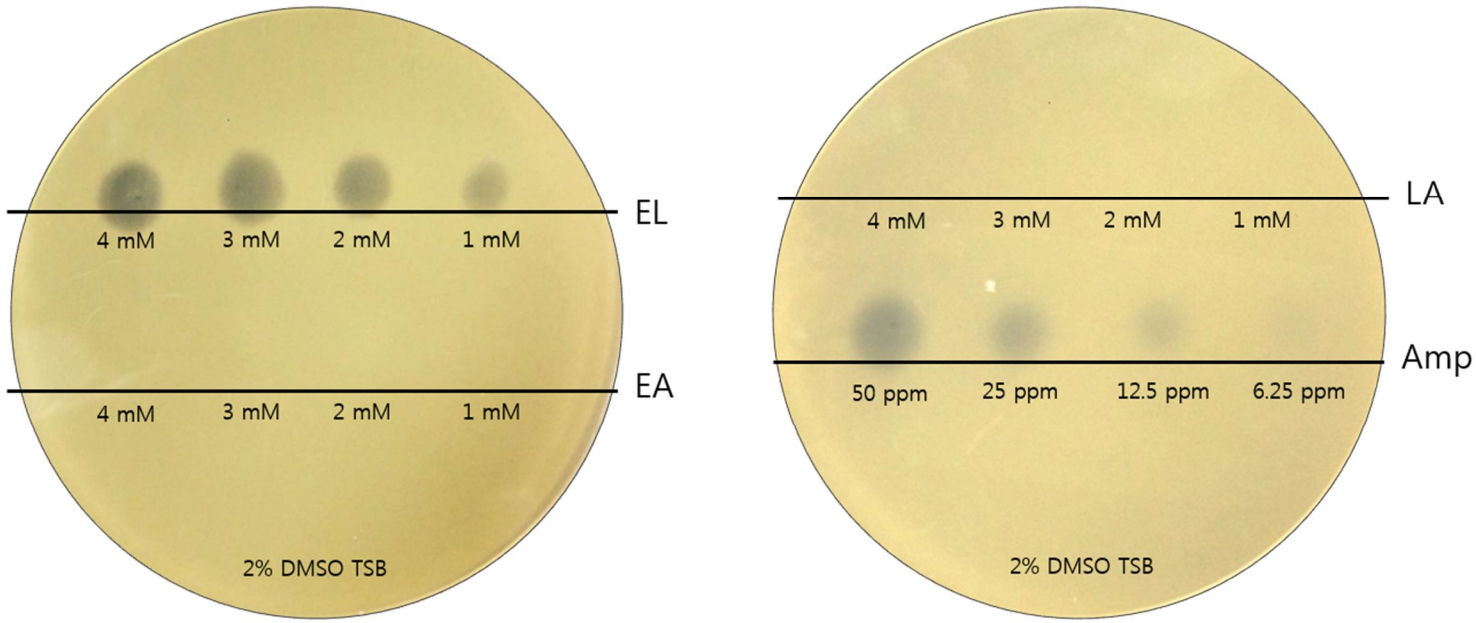

Fig. 1. Antibacterial susceptibility screening of erythorbyl laurate, erythorbic acid, lauric acid, and ampicillin against *Staphylococcus aureus* ATCC 12692.

3-2. Bactericidal and bacteriostatic activity of erythorbyl laurate

3-2-1. Bactericidal activity of erythorbyl laurate

Two gram-negative and two gram-positive bacteria were subject to examine the bactericidal effect of erythorbyl laurate. As a result, gram negative bacteria, *Escherichia coli* ATCC 35150 and *Salmonella* Typhimurium ATCC 19586, did not show any meaningful reduction in viable cells and significant difference in bactericidal effect between erythorbic acid, lauric acid, and erythorbyl laurate (Fig. 2A and 2B). In contrast, it was found that erythorbyl laurate had bactericidal effect on gram positive bacteria, *Listeria monocytogenes* ATCC 19114 and *Staphylococcus aureus* ATCC 27213 (Fig. 2C and 2D). Both *L. monocytogenes* and *S. aureus* showed decrease in the number of viable cells as concentration of erythorbyl laurate increased up to 200 μg/mL. In case of *L. monocytogenes*, the number of viable cells was constant and close to zero above 200 μg/mL. On the other hand, erythorbyl laurate above 200 μg/mL in *S. aureus* showed continuous reduction in viable cells. These results indicated that erythorbyl laurate worked against gram positive bacteria, and showed great reduction in viable cells in *L. monocytogenes* than in *S. aureus* with lower concentration.

(A)

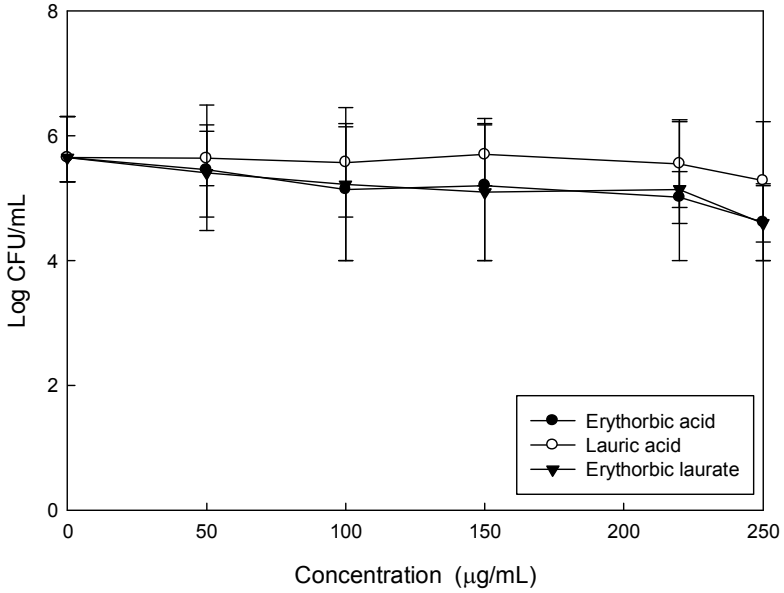
Log CFU/mL
Concentration (μg/mL)
Erythorbic acid
Lauric acid
Erythorbic laurate

(B)

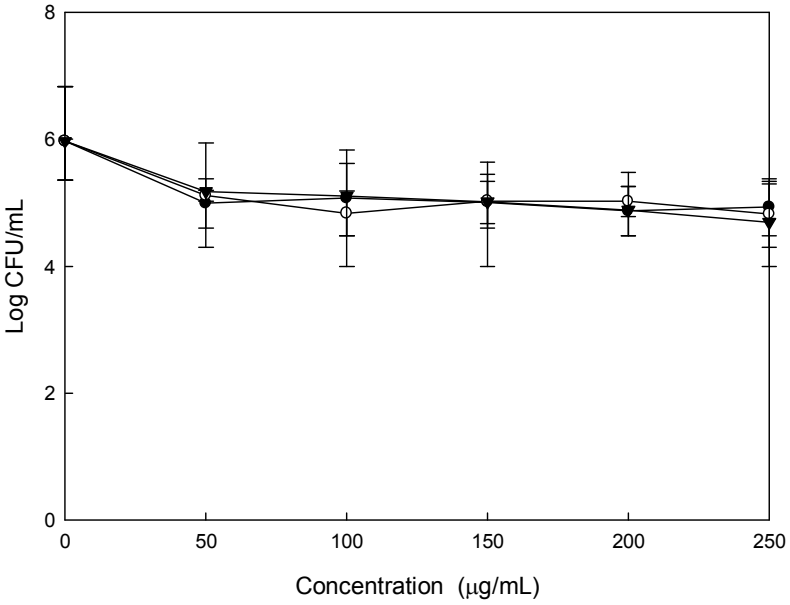
Log CFU/mL
Concentration (μg/mL)

(C)

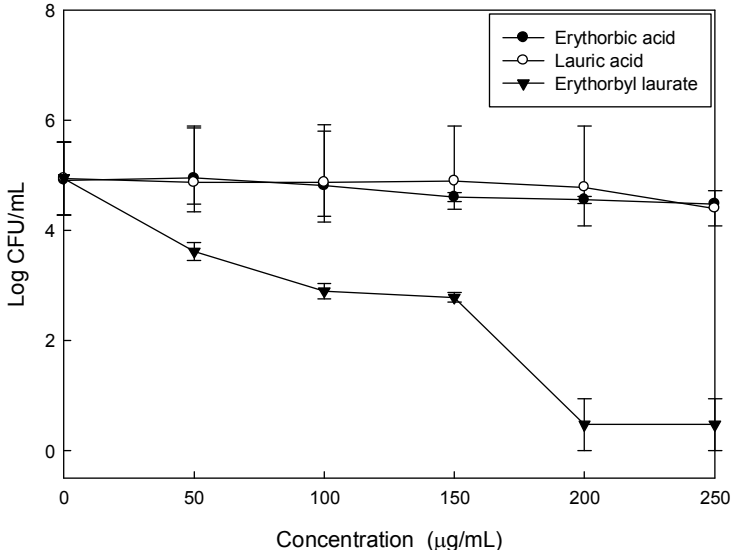

(D)

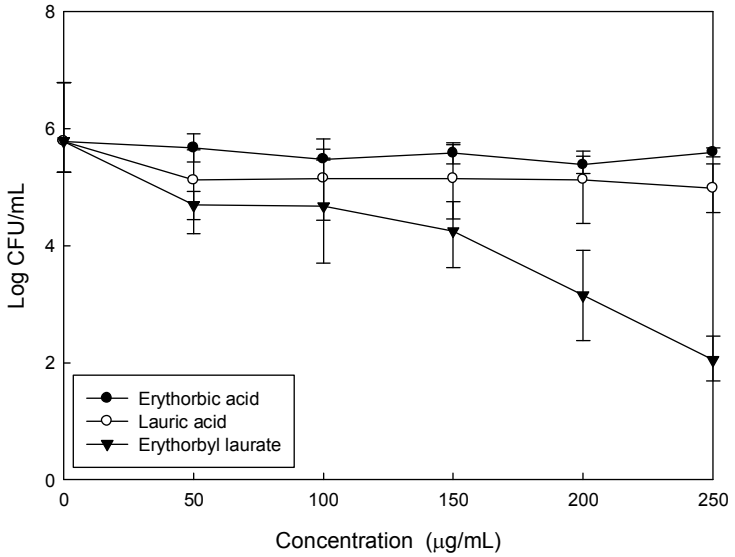

Fig. 2. Bactericidal activity of erythorbyl laurate (▼) against *E. coli* ATCC 35150 (A), *Sal.* Typhimurium ATCC 19586 (B), *L. monocytogenes* ATCC 19114 (C) and *S. aureus* ATCC 27213 (D) compared to erythorbic acid (●) and lauric acid (○).

3-2-2. Minimum inhibitory concentration (MIC) and minimum bactericidal concentration (MBC)

The MICs of erythorbyl laurate for the seven gram positive bacteria strains are shown in Table 1. The MICs were similar between same strains except *S. aureus*. The MICs of erythorbyl laurate for two *S. aureus* ATCC 12692 and ATCC 29213 strains were similar with values of 0.88 mM. But the lowest MIC was observed on *S. aureus* ATCC 49444 with the value of 0.48 mM which was about 2-fold lower than those of other *S. aureus* strains. MBC values were slightly higher than the MICs in most strains. These MIC and MBC values indicated that erythorbyl laurate were mostly bactericidal, but were also bacteriostatic in some cases of low erythorbyl lauarate levels. Bacteriostatic activity of erythorbyl laurate was shown below in 3-4.

Table 1. Minimum inhibitory concentration (MIC) and minimum bactericidal concentration (MBC) of various gram positive bacteria

Bacteria	MIC (mM)	MBC (mM)
S. aureus ATCC 12692	0.88 ± 0.10	1.27 ± 0.12
S. aureus ATCC 29213	0.88 ± 0.10	1.28 ± 0.27
S. aureus ATCC 49444	0.48 ± 0.13	0.80 ± 0.17
B. cereus ATCC 13061	0.73 ± 0.1	0.90 ± 0
B. cereus ATCC 10876	0.65 ± 0.06	1.00 ± 0
L. monocytogenes ATCC 7644	0.58 ± 0.05	0.65 ± 0.07
L. monocytogenes ATCC 19115	0.53 ± 0.15	0.73 ± 0.12

3-2-3. Bacteriostatic activity of erythorbyl laurate

As MIC and MBC results described above, erythorbyl laurate had bacteriostatic effect in some cases of low concentration of erythorbyl lauarate treatments, especially below the MICs. Bacteriostatic effect was demonstrated by lag time ($\Delta\lambda$) and maximum specific growth rate (μ_{max}).

The tendency of lag time ($\Delta\lambda$) and maximum specific growth rate (μ_{max}) were estimated for gram positive bacteria such as *Listeria monocytogenes*, *Bacillus cereus* and *Staphylococcus aureus* in the presence of erythorbyl laurate. As concentration of erythorbyl laurate increased, all tested gram positive bacteria showed increase in lag time ($\Delta\lambda$) and decrease in maximum specific growth rate (μ_{max}) (Fig. 3). Increase in the lag time could be calculated to allow comparison between bacteria strains and concentrations of erythorbyl laurate. The effect of erythorbyl laurate was found to be concentration-dependent, with a major effect of lag time increase at concentrations close to MICs. For example, at 0.6 mM, *S. aureus* ATCC 12692 and ATCC 29213 showed 1.5 and 0.5 h of increase in lag time, respectively, and at the concentration below 4-fold diluted sub-MIC concentrations, a relatively small increase in lag time was observed. As shown in Table 2, it was found that there was similar trend between *S. aureus* and *B. cereus* that significant increase in lag time started at approximate

concentration of MIC. For *L. monocytogenes*, a different trend was detected, with a more gradual increase in lag time with an effect observed even at 8-fold sub-MIC. It is plausible to assume that the bacteriostatic activity arises from the extension of lag phase, because the increase in lag time was proportional to the concentration of erythorbyl laurate. Meanwhile, compared to other lauric acid-related antimicrobial agent such as lauric acid and ascorbyl laurate, it is worthy of attention that erythorbyl laurate showed greater antimicrobial activity than that of lauric acid (Fig. 4). These results showed that antimicrobial activity of esterification between erythorbic acid and lauric acid had better synergistic effect than between ascorbic acid and lauric acid.

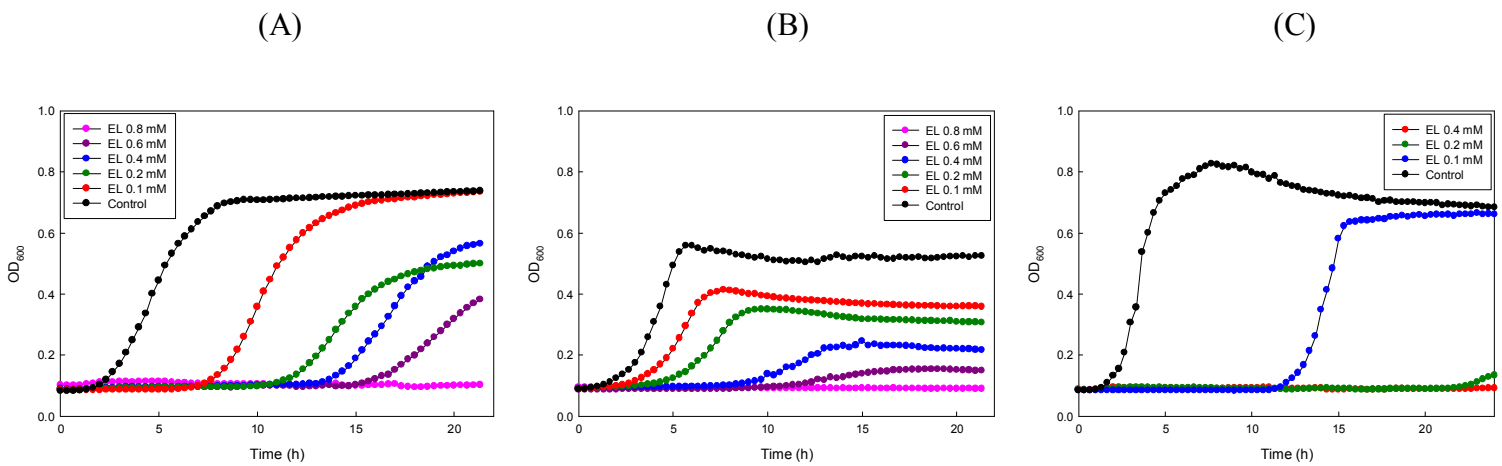

Fig. 3. Growth curve of gram positive bacteria, *S. aureus* ATCC 12692 (A), *L. monocytogenes* ATCC 7644 (B) and *B. cereus* ATCC 10876 (C) treated with serial diluted erythorbyl laurate (EL).

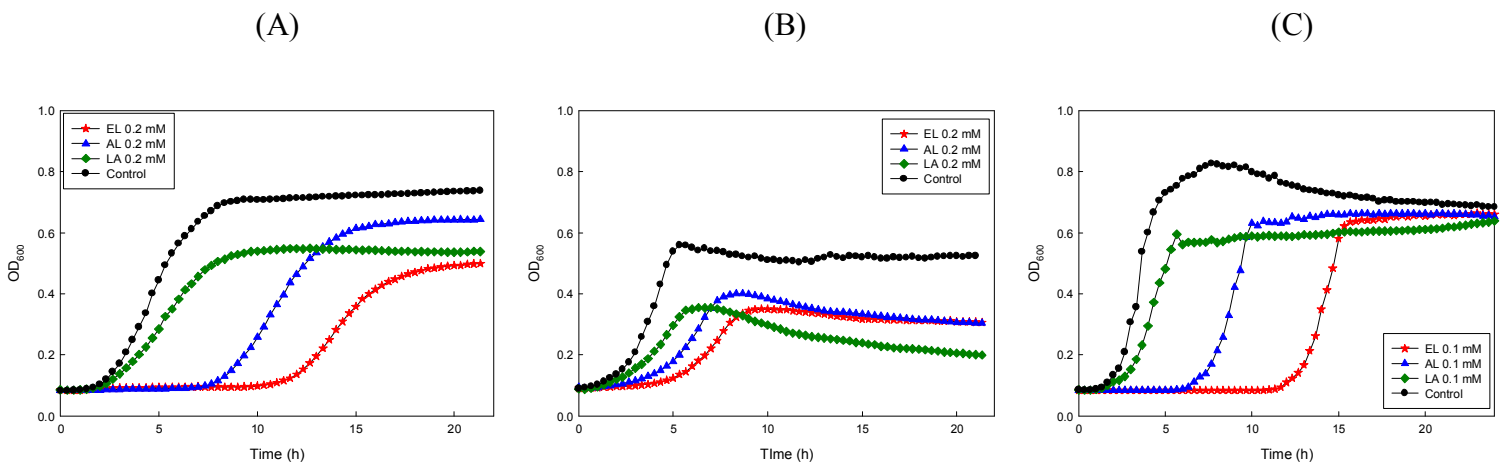

Fig. 4. Growth curve of gram positive bacteria, *S. aureus* ATCC 12692 (A), *L. monocytogenes* ATCC 7644 (B) and *B. cereus* ATCC 10876 (C) treated same concentration of erythorbyl laurate (EL) compared to ascorbyl laurate (AL) and lauric acid (LA).

Table 2. Increase in lag time ($\Delta\lambda$) and decrease in maximum specific growth rate (μ_{max}) for gram positive bacteria depending on the sub-MIC of erythorbyl laurate

Bacteria	**Concentration (mM)**	**Lag time (h)**	**μ_{max} (OD_{600}/h^{-1})**
S. aureus ATCC 12692	0.6	4.50 ± 1.00	0.050 ± 0.002
	0.4	3.33 ± 0.58	0.083 ± 0.003
	Control	3.00 ± 0.58	0.123 ± 0.003
S. aureus ATCC 29213	0.6	2.83 ± 0.87	0.070 ± 0.001
	0.4	2.50 ± 0.58	0.092 ± 0.003
	Control	2.33 ± 0.50	0.149 ± 0.004
S. aureus ATCC 49444	0.4	9.33 ± 0.29	0.019 ± 0.008
	0.2	3.83 ± 0.58	0.055 ± 0.005
	Control	3.17 ± 2.02	0.090 ± 0.005
B. cereus ATCC 13061	0.4	5.33 ± 1.44	0.034 ± 0.012
	0.2	2.50 ± 1.32	0.078 ± 0.006
	Control	2.00 ± 0.58	0.190 ± 0.008
B. cereus ATCC 10876	0.4	4.50 ± 2.02	0.033 ± 0.003
	0.2	2.67 ± 0.00	0.077 ± 0.011
	Control	2.17 ± 0.29	0.137 ± 0.006
L. monocytogenes ATCC 7644	0.4	6.50 ± 0.00	0.011 ± 0.009
	0.2	4.50 ± 0.87	0.028 ± 0.009
	Control	3.00 ± 0.29	0.091 ± 0.012
L. monocytogenes ATCC 19115	0.4	7.50 ± 0.29	0.004 ± 0.003
	0.2	5.50 ± 0.29	0.026 ± 0.004
	Control	3.25 ± 0.71	0.094 ± 0.004

3-3. Change in cell permeability

After incubation with pre-determined concentrations of erythorbyl laurate, crystal violet uptakes were measured with a spectrophotometer at 590 nm. All tested bacteria, *S. aureus* ATCC 12692, ATCC 29213, and ATCC 49444 showed increased crystal violet uptakes up to 1.6, 2.0, and 1.2 mM of erythorbyl laurate (Fig. 5). On the other hand, above these concentrations, crystal violet uptakes decreased as the concentration of erythorbyl laurate increased. It could be the results from disintegration of cell membrane and released nucleic acid stained with crystal violet. Meanwhile, samples treated with positive control, nisin (40 mg/mL), of which mechanism was inducing pore formation on membranes showed 81.8, 81.0, and 79.8% of crystal violet uptakes of each tested bacteria, respectively. These increasing trend of permeability was similar to that of crystal violet uptake levels of each bacteria samples treated with erythorbyl laurate until the crystal violet uptake levels reached to maximum values. On the other hand, all bacteria samples with another positive control, ampicillin (50 μg/mL) which is known to inhibit cell wall synthesis, had similar crystal violet uptakes compared to the untreated control sample, corresponding to 17.25, 35.75, and 17.9%, respectively. It indicated that erythorbyl laurate had similar mechanism with nisin, rather than ampicillin.

(A)

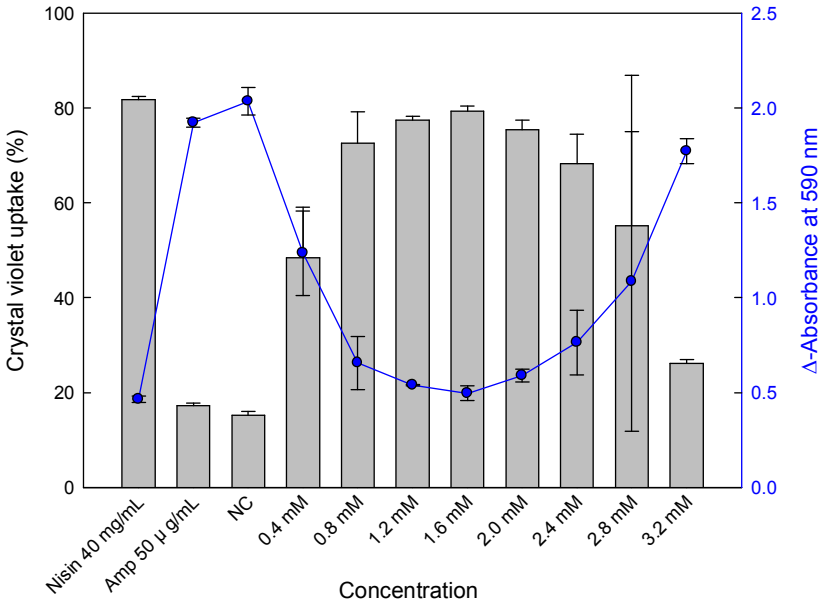
Crystal violet uptake (%)
Δ-Absorbance at 590 nm
Concentration
Nisin 40 mg/mL
Amp 50 μg/mL
NC
0.4 mM
0.8 mM
1.2 mM
1.6 mM
2.0 mM
2.4 mM
2.8 mM
3.2 mM

(B)

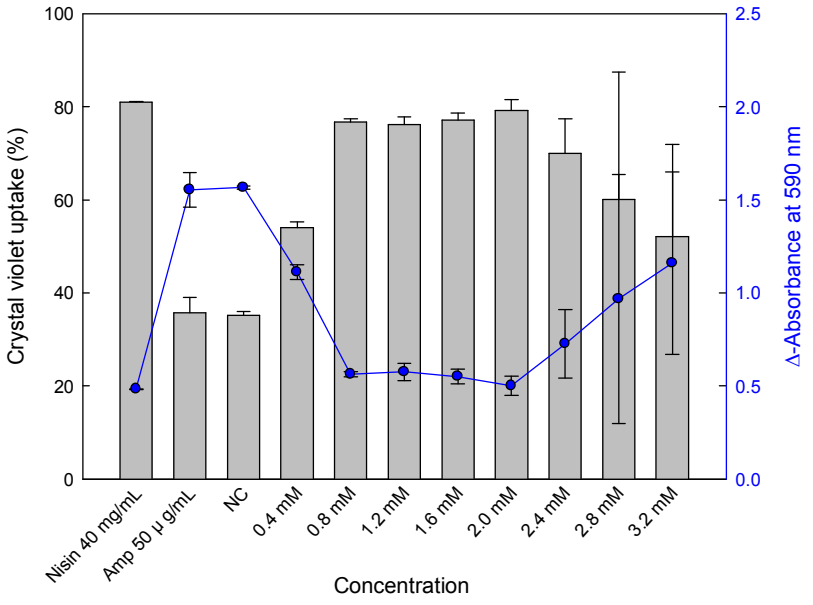
Crystal violet uptake (%)
Δ-Absorbance at 590 nm
Concentration
Nisin 40 mg/mL
Amp 50 μg/mL
NC
0.4 mM
0.8 mM
1.2 mM
1.6 mM
2.0 mM
2.4 mM
2.8 mM
3.2 mM

(C)

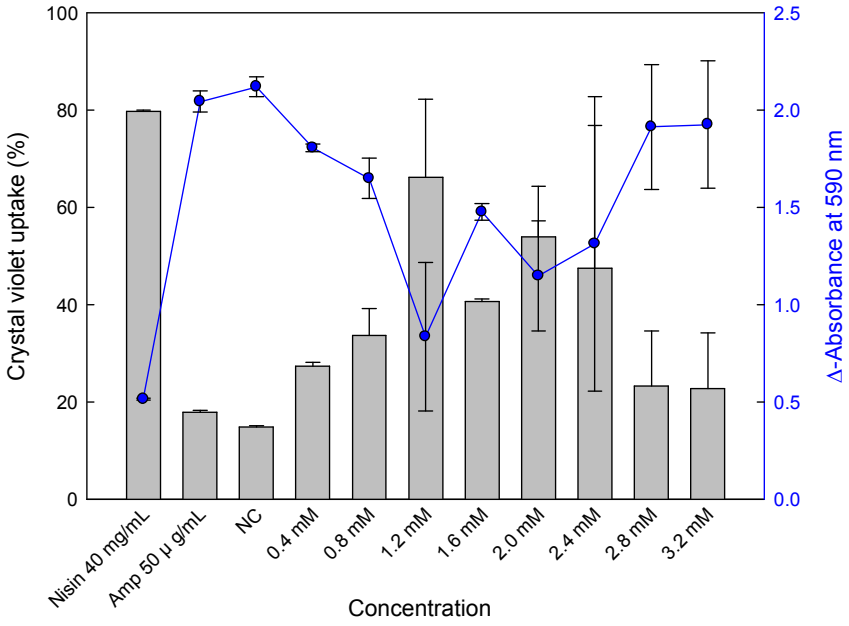

Fig. 5. Crystal violet uptake (%) representing cell permeability ( ) and Δ-absorbance of crystal violet at 590 nm (–) of *S. aureus* ATCC 12692 (A), *S. aureus* ATCC 29213 (B) and *S. aureus* ATCC 49444 (C).

3-4. Assessment of cell rupture with fluorescence

3-4-1. Evaluation of the percentage of *S. aureus* with damaged membrane

Bacteria membrane rupture was further assessed by using the Live/Dead BacLight viability kit which uses dyes, SYTO 9 that stains both intact and damaged cells and propidium iodide that enters cell and stains cellular DNA only if the membrane is damaged and permeable. The fluorescence intensities of the stained bacterial suspension at 530 nm (green, G) and 630 nm (red, R) directly proportional to the numbers of live and dead cells, respectively. Standard curve was plotted by the fluorescence Ratio $_{G/R}$ of standard curve samples and relative live percentage of bacterial suspension treated by erythorbyl laurate was obtained through the Ratio $_{G/R}$. Exposure of *S. aureus* to erythorbyl laurate at various concentrations showed altered relative live percentage which was regarded as relative number of bacteria cells with intact cytoplasmic membrane (Fig. 6). It revealed that there was rapid reduction of relative live percentage at around MICs of each *S. aureus* strain. Strain ATCC 12692, ATCC 29213 and ATCC 49444 reached 0% of relative live percentage at the concentrations above 1.2, 1 and 0.9 mM, respectively. Unidentified increase in the relative live percentage at sub-MIC concentration seemed to be related with increase in permeability of SYTO 9

dye, which was dominant in relative live percentage at low concentration of erythorbyl laurate (Stocks, 2004).

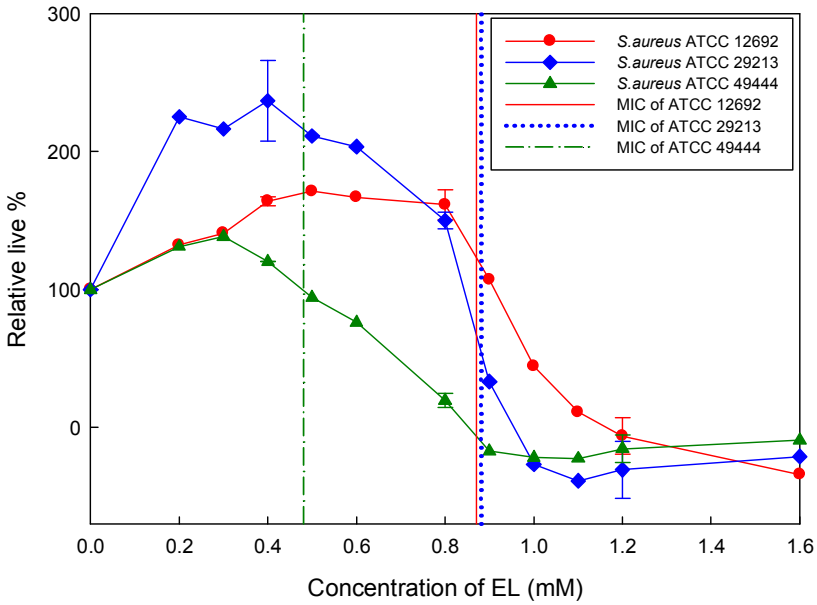

Fig. 6. Effect of erythorbyl laurate at various concentration on membrane integrity in *S. aureus* ATCC 12692 (●), ATCC 29213 (◆), and ATCC 49444 (▲). Relative live percentage was calculated by using the standard curve of the Ratio $_{G/R}$ versus the percentage of live cells.

3-4-2. Visualized images of cell rupture evidence by fluorescence microscopy

To further verify the results of Fig. 6, fluorescence microscopy was performed with Live/Dead viability kit. Fluorescence micrographs of stained bacteria suspension without erythorbyl laurate treatment showed little red cells stained with propidium iodide (Fig. 7A). However, samples treated with 1×MIC and 2×MIC of erythorbyl laurate fluoresced both green and red so that showed yellow in overlay (Fig. 7B and 7C). The number of cells stained only green dye with intact membrane was decreased as concentration of erythorbyl laurate increased, and it revealed that 2×MIC of erythorbyl laurate treatment inhibited almost all cells because of membrane rupture.

(A)

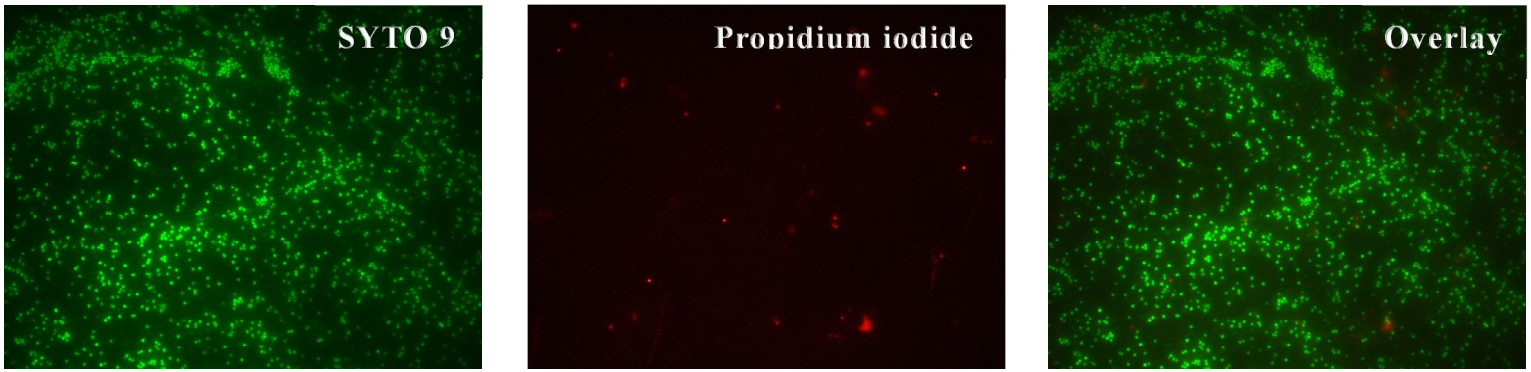
SYTO 9
Propidium iodide
Overlay

(B)

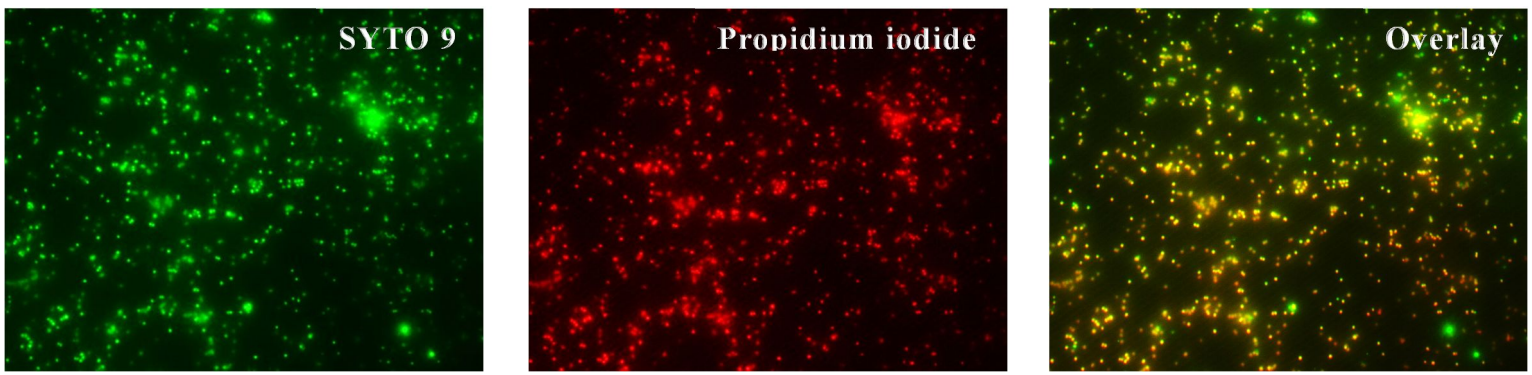
SYTO 9
Propidium iodide
Overlay

(C)

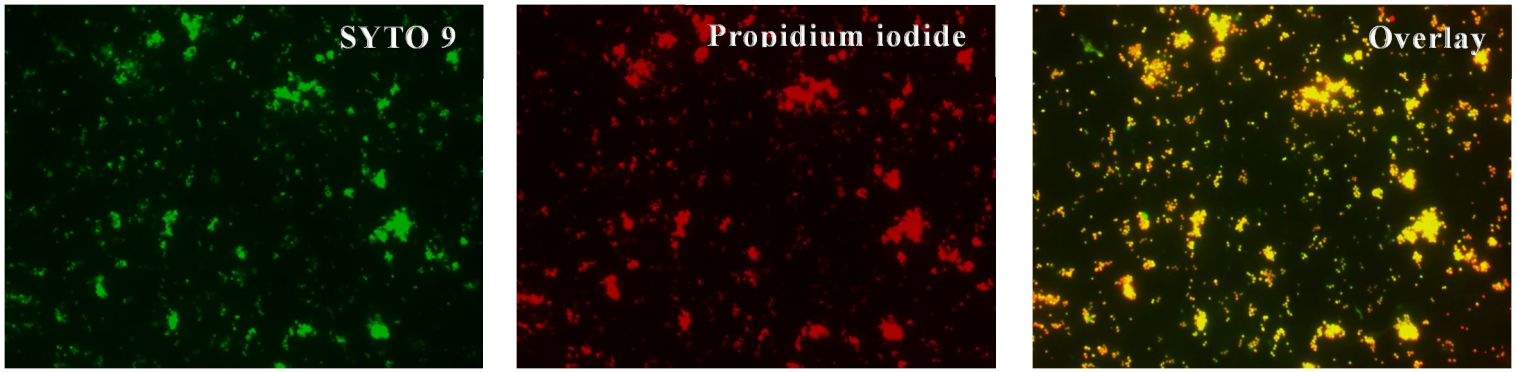

Fig. 7. Overlay of SYTO 9 and propidium iodide fluorescence images of cells without erythorbyl laurate (A), treated with 1×MIC (B) and treated with 2×MIC (C). SYTO 9 stained both intact and damaged cells, and cells with compromised membranes were stained only with propidium iodide (red).

3-5. Morphological characterization of bacterial cell rupture by erythorbyl laurate

EF-TEM was performed to assess any structural differences in the bacterial cells following exposure to inhibitory and bactericidal erythorbyl laurate concentration. *S. aureus* ATCC 29213 was treated with MIC and 4-fold MIC of erythorbyl laurate for 12 h. These electron micrographs of bacteria sample without erythorbyl laurate treatment showed that bacteria retained the integrality of plasma membrane. In contrast, samples treated with MIC and 4-fold MIC of erythorbyl laurate showed slight leakages of cellular cytoplasmic contents and a variety of membrane perturbations were observed. At the concentration of MIC, membrane roughening and slight cytoplasmic convolution were notable as indicated by cytoplasmic membrane boundary becoming faint. Moreover, membrane of bacteria treated with 4-fold MIC of erythorbyl laurate was completely ruptured, accompanied by significant release of cellular contents. EF-TEM images of *S. aureus* ATCC 29213 interacting with erythorbyl laurate at inhibitory and bactericidal concentrations indicated that erythorbyl laurate addition caused dissolution of the cytoplasmic space, significant roughing of the membrane, and cytoplasmic convolution within 12 h of exposure. When the membrane and cell wall of bacteria were damaged by erythorbyl laurate, there were

intracellular components released from the cells and increasing permeability and the results from the crystal violet assay and Live/Dead bacLight kit assay could also verified these results. These changes in the cell wall and membrane could be a major factor in killing by erythorbyl laurate.

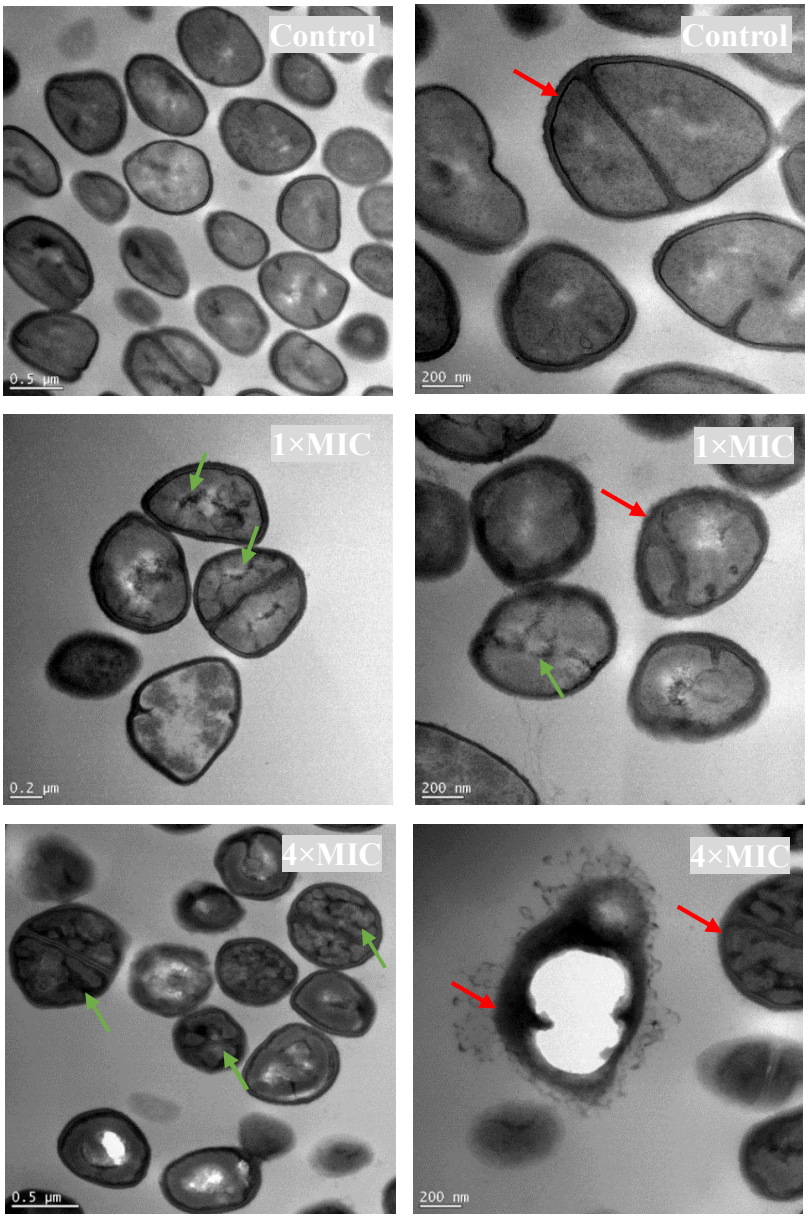

Fig. 8. Transmission electron micrographs of *S. aureus* ATCC 29213 treated with 1×MIC and 4×MIC of erythorbyl laurate for 12 h. It revealed that cell envelop rupture (→) and cytoplasmic disorder (→).

3-6. Synergistic effect with antibiotics and food additives

The combined effect of commercial antimicrobial agents and erythorbyl laurate was evaluated against *S. aureus* ATCC 29213. The FIC index of combination of erythorbyl luarate and other antimicrobial agents was evaluated by the checkerboard test, and the results were shown in Table 3. For *S. aureus* ATCC 29213, the FIC index of erythorbyl laurate with nisin, ampicillin, kanamycin, erythromycin, chloramphenicol, and streptomycin were lower than 0.5 which represented a synergistic interaction. In particular, nisin, kanamycin, and erythromycin showed great synergistic effect with erythorbyl laurate. The rest antimicrobial agents which showed indifferent effect with erythorbyl laurate also had possibility to decrease the amount of other antimicrobial agents used and riskiness of antibiotics-resistant pathogens (Fig. 9). It revealed that erythorbyl laurate had strong point in the way that raised effect of other antimicrobial agents during treatments.

Table 3. Fractional inhibitory concentration (FIC) index of erythorbyl laurate and other antimicrobial agents against *S. aureus* ATCC 29213

Target mechanism	Name	∑FIC	Effect
Electron transport system	Potassium sorbate	1.25	Indifferent
Interference with the permeability of the cytoplasmic membrane by rupturing	Nisin	<0.281	Synergistic
Cell wall synthesis	Cephalexin	0.75	Indifferent
	Ampicillin	0.5	Synergistic
	Cloxacillin	1.25	Indifferent
Protein synthesis	Sodium benzoate	0.75	Indifferent
	Kanamycin	0.256	Synergistic
	Erythromycin	0.266	Synergistic
	Chloramphenicol	0.5	Synergistic
	Streptomycin	0.5	Synergistic
DNA/RNA synthesis	Nalidixic acid (DNA)	0.75	Indifferent
	Rifampicin (RNA)	0.75	Indifferent

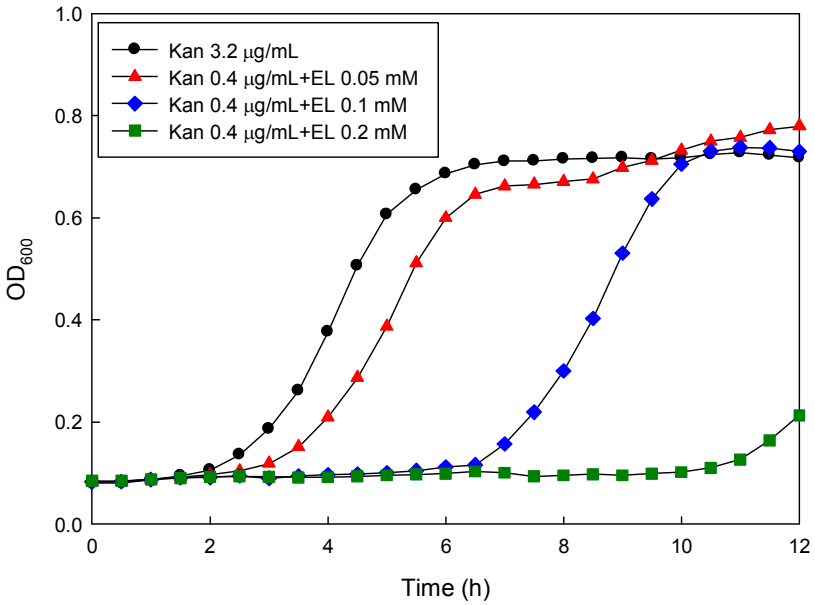

Fig. 9. Growth curve of *S. aureus* ATCC 29213 treated serial diluted erythorbyl laurate and kanamycin in combination.

3-7. Transcriptional analysis by RNA-Seq

Exponentially growing *S. aureus* Newman were challenged with 0.1 mM sub-MIC concentration of erythorbyl laurate which slightly inhibited growth but did not show bactericidal activity for 15 min. Gene expression changes in the erythorbyl laurate treated cells as compared to non-treated cells were analyzed by RNA-Seq. There were large numbers of up-regulated genes and down-regulated genes from a variety of functional categories (Table 4 and Table 5) induced by erythorbyl laurate. Previous transcriptional profiling studies of the response of *S. aureus* revealed the induction of a cell wall stress stimulon by cell wall-active agents (Kuroda, Kuroda, Oshima, Takeuchi, Mori, & Hiramatsu, 2003; Utaida, Dunman, Macapagal, Murphy, Projan, Singh, et al., 2003; Wilkinson, Muthaiyan, & Jayaswal, 2005). Many of these genes are regulated by two-component system composed of a response regulator, VraR and a sensor, VraS. Erythorbyl laurate treatment showed up-regulation in both the *vraR* and *vraS* genes. Correlated changes in other cell wall stress stimulon genes were also observed upon erythorbyl laurate treatment. Several genes under VraSR control, such as *vraS, vraR, prsA, dapA, asd, cysM, thrC, ilvE, drp35*, and MerR family regulatory protein (NWMN_2290), were all up-regulated by erythorbyl laurate.

Compared erythorbyl laurate with other strong cell wall-active antibiotics including vancomycin, oxacillin, and daptomycin, *vraS* and *vraR* were up-regulated by all these antimicrobial agents, but there were differences between the erythorbyl laurate and other cell wall-active agents in expression levels of VraSR and presence of expressed genes related cell wall-active stimulons such as *murAB, pbpB, tcaA*, various *tag* genes, r*ecU*, and *spsB* (Kuroda, Kuroda, Oshima, Takeuchi, Mori, & Hiramatsu, 2003).

Meanwhile, large numbers of genes in various categories were down-regulated by erythorbyl laurate. There were several down-regulated genes related with energy metabolism, translation, nucleic acid metabolism, transporter and binding proteins, and these patterns were shown at the transcriptional analysis with nisin-treated *S. aureus*. It has been proposed that nisin inserts into the membrane and forms pores, resulting in depolarization of the membrane and the rapid efflux of cytoplasmic ions, amino acids, and nucleotides (Driessen, van den Hooven, Kuiper, Van de Camp, Sahl, Konings, et al., 1995; Muthaiyan, Silverman, Jayaswal, & Wilkinson, 2008).

As discussed above, erythorbyl laurate had a similarity with cell wall-active and membrane-depolarizing antimicrobial agents in changes of gene expression. It seemed that transcriptional profiling verified these potential dual mode of action, of erythorbyl laurate.

Table 4. Expression of genes up-regulated by erythorbyl laurate

Gene ID	Gene name	Protein	Expression change	Category
Cell envelope				
5331053		Glycosyltransferase	3.8	Peptidoglycan biosynthesis
5331236	murZ	UDP-*N*-acetylglucosamine 1-carboxyvinyltransferase	2.9	Peptidoglycan biosynthesis
5331477	fnbA	Fibronectin binding protein A precursor	2.7	Peptidoglycan-anchor
5331791	capB	Capsular polysaccharide synthesis enzyme CapB	2.7	External encapsulating structure organization
5331797	capE	Capsular polysaccharide biosynthesis protein CapE	2.3	External encapsulating structure organization
5331802	capI	Capsular polysaccharide biosynthesis protein CapI	2.1	External encapsulating structure organization
5331985	engB	Ribosome biogenesis GTP-binding Protein YsxC	2.6	Cell cycle and division
5330218	lpl1nm	Tandem lipoprotein	4.6	Cell membrane proteins
5332092	lpl4nm	Tandem lipoprotein	4.3	Cell membrane proteins
5332094	lpl6nm	Tandem lipoprotein	3.3	Cell membrane proteins
5330219	lpl3nm	Tandem lipoprotein	3.0	Cell membrane proteins
5332093	lpl5nm	Tandem lipoprotein	2.6	Cell membrane proteins
5330179	tatA	Twin-arginine translocation protein TatA	2.8	Cell membrane proteins
5332033	icaA	*N*-glycosyltransferase	2.5	Cell membrane proteins
Amino acid biosynthesis				
5331999	hisC	Histidinol-phosphate aminotransferase	6.9	Nitrogen compound biosynthetic process

5332564	trpC	Indole-3-glycerol-phosphate synthase	4.8	Nitrogen compound biosynthetic process
5332003	hisA	1-(5-phosphoribosyl)-5-[(5-phosphoribosylamino)methylideneamino] imidazole-4-carboxamide isomerase	4.8	Nitrogen compound biosynthetic process
5331741	argR	Arginine repressor	4.3	nitrogen compound biosynthetic process
5330228	cysM	Cysteine synthase	4.0	nitrogen compound biosynthetic process
5330774	lysC	Aspartate kinase	15.2	Lysine biosynthesis
5332108	asd	Aspartate semialdehyde dehydrogenase	10.6	Lysine biosynthesis
5331853	dapB	Dihydrodipicolinate reductase	8.8	Lysine biosynthesis
5331759	dapA	Dihydrodipicolinate synthase	7.8	Lysine biosynthesis
5331854	dapD	Tetrahydrodipicolinate acetyltransferase	6.1	Lysine biosynthesis
5332450	sbnH	Diaminopimelate decarboxylase	2.5	Lysine biosynthesis
5331732	lysA	Diaminopimelate decarboxylase	3.7	Lysine biosynthesis
5332539	metL	Homoserine dehydrogenase	4.5	Lysine, branched-chain amino acid biosynthesis
5332039	leuA	2-Isopropylmalate synthase	3.2	branched-chain amino acid biosynthesis
5332038	ilvC	Ketol-acid reductoisomerase	2.8	branched-chain amino acid biosynthesis
5331962	gltD	Glutamate synthase subunit beta	3.5	Alanine, aspartate and glutamate metabolism
5332079	leuD	Isopropylmalate isomerase small subunit	2.7	branched-chain amino acid biosynthesis
5332078	leuC	Isopropylmalate isomerase large subunit	2.6	branched-chain amino acid biosynthesis
5332077	leuB	3-Isopropylmalate dehydrogenase	2.5	branched-chain amino acid biosynthesis
5332541	thrB	Homoserine kinase	2.7	Glycine, serine and threonine metabolism
5332129	thrC	Threonine synthase	2.5	Glycine, serine and threonine metabolism

Protein fate

5331192		Iron compound ABC transporter iron compound-binding protein	6.3	Metal ion transmembrane transporter activity
5332448	sbnF	Siderophore biosynthesis IucC family protein	4.4	Metal ion transmembrane transporter activity
5331103	pepS	Aminopeptidase PepS	5.6	Peptidase activity
5331103	pepS	Aminopeptidase PepS	5.6	Peptidase activity
5331855	hipO	Hippurate hydrolase	3.8	Peptidase activity
5332332		Type III leader peptidase family protein	3.0	Peptidase activity
5331023	prsA	Peptidyl-prolyl cis/trans-isomerase	3.2	Protein folding & chaperone
5331929	hslO	Hsp33-like chaperonin	2.7	Protein folding & chaperone
5331387		Acetyltransferase, GNAT family protein	3.1	N-acetyltransferase activity
5330314		Acetyltransferase, GNAT family protein	2.9	N-acetyltransferase activity
5331371		Drug resistance transporter EmrB/QacA subfamily protein	2.7	Drug transporter activity
5332032	icaB	Intercellular adhesion protein B	6.1	Signal peptide
5331477	fnbA	Fibronectin binding protein A precursor	2.7	Signal peptide

Cellular processes

5332008	hlgC	Gamma-hemolysin component C	10.4	Cytolysis of cells of another organism
5332104	lukS	Leukocidin/hemolysin toxin subunit S	8.6	Cytolysis of cells of another organism
5331190	lukF	Leukocidin/hemolysin toxin subunit F	7.8	Cytolysis of cells of another organism
5332443	hlgA	Gamma-hemolysin component A	7.1	Cytolysis of cells of another organism
5332010	hlgB	Gamma hemolysin, component B	6.9	Cytolysis of cells of another organism
5331610	drp35	Drp35	8.6	Metal ion binding, response to antibiotic
5332445	sbnC	Siderophore biosynthesis IucC family protein	4.8	Metal ion binding, response to antibiotic

5331606		ABC transporter ATP-binding protein	4.3	ATP, adenyl nucleotide binding
5330486		NADH-dependent flavin oxidoreductase	4.3	Nuleotide, cofactor binding
5330536		Lipoate-protein ligase A	2.7	Nucleotide, ATP-binding
5331248		Zinc and cobalt transport repressor protein	2.6	Winged helix repressor DNA-binding
5331888	ipdC	Indole-3-pyruvate decarboxylase	2.6	Cofactor binding
5331959	glpD	Aerobic glycerol-3-phosphate dehydrogenase	3.5	Nucleotide phosphate-binding region:FAD
5330424	trxB	Thioredoxin reductase	2.8	Nucleotide phosphate-binding region:FAD, electron carrier activity
5331258		Arginase	2.6	Arginine and proline metabolism, metal ion binding
5331746	argD	Ornithine aminotransferase	4.1	Arginine and proline metabolism
5329983	aldA	Aldehyde dehydrogenase-like protein	4.3	Glycerolipid metabolism, oxidoreductase activity
5332031	lip	Lipase precursor	3.1	Glycerolipid metabolism
5332483	set9nm	Superantigen-like protein	3.7	Staphylococcal toxin
5332480	set6nm	Superantigen-like protein	2.5	Staphylococcal toxin
5331488	fbp	Fructose-1,6-bisphosphatase	3.6	Carbohydrate biosynthetic process
5331907	acs	Acetyl-CoA synthetase	3.5	Glycolysis / Gluconeogenesis
5331997	alr2	Alanine racemase 2	3.5	Pyridoxal phosphate
5330989		Putative translaldolase	2.9	Pentose phosphate pathway
5331971	gntK	Gluconate kinase	2.7	Pentose phosphate pathway
5331430		Amino acid permease	2.7	Amino acid transporter
5331898		Acetyl-CoA/acetoacetyl-CoA transferase	7.1	

5330680		Putative transposase	5.6	
5331783	bsaA2	Lantibiotic precursor	4.7	
5331829	fadA	Acetyl-CoA acetyltransferase-like protein	4.5	
5331489		Phospholipase/carboxylesterase family protein	3.5	
5330230		ABC transporter substrate-binding protein	2.7	
5329997	entB	Isochorismatase	2.7	
5330500		Truncated MHC class II analog protein	2.5	
Regulatory functions				
5331535		Transcriptional regulator TetR family protein	3.4	Regulation of transcription, DNA-dependent
5331549		Transcriptional regulator TetR family protein	3.0	Regulation of transcription, DNA-dependent
5331404		MerR family regulatory protein	3.0	Regulation of transcription, DNA-dependent, negative regulation of macromolecule biosynthetic process
5331741	argR	Arginine repressor	4.3	Winged helix repressor DNA-binding
5330495		LysR family regulatory protein	3.0	Winged helix repressor DNA-binding
Signal transduction				
5332564	trpC	Indole-3-glycerol-phosphate synthase	4.8	Two-component systems
5332602	vraS	Sensor histidine kinase VraS	2.1	Two-component systems
5331107	vraR	DNA-binding response regulator VraR	3.5	Two-component systems

*Bolded gene IDs were related with dual-mechanism of erythorbyl laurate.

Table 5. Expression of genes down-regulated by erythorbyl laurate

Gene ID	Gene name	product	Expression change	Category
Cell envelope				
5331038		Extracellular glutamine-binding protein	-4.2	peptidoglycan-based cell wall
5330047	scdA	Cell wall biosynthesis protein ScdA	-2.8	cell division
5331856		Cell division protein	-2.6	cell division
5332180	murE	UDP-N-acetylmuramoylalanyl-D-glutamate--L-lysine ligase	-2.3	peptidoglycan biosynthesis
5331865	dltD	D-alanine-activating DltD protein	-2.1	D-alanylation
Amino acid biosynthesis				
5331750	argG	Argininosuccinate synthase	-19.5	Nitrogen compound biosynthetic process
5331961	argH	Argininosuccinate lyase	-16.5	Nitrogen compound biosynthetic process
5330838		Pyrroline-5-carboxylate reductase	-5.7	Nitrogen compound biosynthetic process
5332191		Nnitric oxide synthase oxygenase	-3.6	Nitrogen compound biosynthetic process
5329996	argJ	Bifunctional ornithine acetyltransferase/N-acetylglutamate synthase	-2.6	Nitrogen compound biosynthetic process
5331561		Glycine betaine aldehyde dehydrogenase	-4.1	Nitrogen compound biosynthetic process
5332342	ahrC	Arginine repressor	-2.5	arginine biosynthesis
Protein function				
5331527		Immunodominant antigen A	-10.9	extracellular region signal peptide
5332586	ureG	Urease accessory protein UreG	-4.7	nucleotide-binding
5331747		Branched-chain amino acid transport system II carrier protein	-4.2	amino acid transmembrane transporter activity

5330693	rpmB	50S ribosomal protein L28	-3.6	translation
5331492		Acetyltransferase, GNAT family protein	-3.2	N-acetyltransferase activity
5331526		Acetyltransferase, GNAT family protein	-2.6	N-acetyltransferase activity
5330883	rpsU	30S ribosomal protein S21	-3.2	translation
5332532	rpmE2	50S ribosomal protein L31 type B	-2.6	translation
5331300	rpsL	30S ribosomal protein S9	-2.5	translation
5330887	rpsT	30S ribosomal protein S20	-2.5	translation
5331354		Peptidase M20/M25/M40 family protein	-3.0	peptidase activity
5332558	rplS	50S ribosomal protein L19	-2.5	structural constituent of ribosome
Cellular processes				
5330168		Glycerol-3-phosphate transporter	-4.8	carbohydrate transport
5330048		PTS system, IIA component	-4.7	carbohydrate transport
5332334	rbsU	Ribose transporter RbsU	-3.1	carbohydrate transport
5332223		Oligopeptide transport system permease	-4.7	cell membrane
5330797		Cell wall associated fibronectin-binding protein	-2.6	cell membrane
5332479	set5nm	Superantigen-like protein 5	-4.5	Staphylococcus aureus exotoxin
5330660	hla	Alpha-hemolysin precursor	-2.6	cytolysis of cells of another organism
5329981	adhE	Bifunctional acetaldehyde-CoA/alcohol dehydrogenase	-4.5	oxidoreductase activity
5331561		Glycine betaine aldehyde dehydrogenase	-4.1	oxidoreductase activity
5330560	qoxD	Quinol oxidase polypeptide IV	-3.9	cytochrome-c oxidase activity
5332329	qoxC	Quinol oxidase polypeptide III	-3.3	cytochrome-c oxidase activity
5332221	opp1C	Oligopeptide transporter putative membrane permease	-3.3	ABC transporters
5332173	fmtB	Methicillin resistance determinant FmtB	-3.1	Gram-positive signal peptide

		protein		
5330374		Anion transporter family protein	-3.2	monovalent inorganic cation transport
5331356	fofB	Fosfomycin resistance protein FosB	-3.2	response to antibiotic
5329920	hutH	Histidine ammonia-lyase	-4.0	Histidine metabolism
5331808	capO	Capsular polysaccharide biosynthesis protein CapO	-3.1	Amino sugar and nucleotide sugar metabolism
5330023	pflB	Formate acetyltransferase	-3.0	Pyruvate, Propanoate, Butanoate, propanoate metabolism
5332182	fbaA	Fructose-bisphosphate aldolase	-2.7	Fructose and mannose metabolism
5330952	plsC	1-acyl-sn-glycerol-3-phosphate acyltransferase	-2.7	Glycerolipid metabolism
5329990		Formate dehydrogenase	-2.9	cofactor binding
5331795	capB	Polysaccharide biosynthesis protein CapD	-2.5	cofactor binding
5332135	mnhB	Putative monovalent cation/H+ antiporter subunit B	-2.9	metal ion binding protein
5331565		Anaerobic ribonucleotide reductase, small subunit	-2.7	metal cluster binding
5331439		General substrate transporter involved in chloramphenicol resistance	-2.6	Major facilitator superfamily MFS-1
Regulatory functions				
5331138		ABC transporter ATP-binding protein	-10.7	nucleotide-binding
5331217	kdpC	Potassium-transporting ATPase subunit C	-5.3	nucleotide-binding
5331139		GntR family regulatory protein	-5.0	Winged helix repressor DNA-binding
5331485		Transcriptional regulator MarR family protein	-4.2	Winged helix repressor DNA-binding
5331029		DNA-binding response regulator	-2.9	Winged helix repressor DNA-binding

5331400		MarR family regulatory protein	-2.9	Winged helix repressor DNA-binding
5332100		Transcriptional regulator, GntR family protein	-2.8	Winged helix repressor DNA-binding
5329969	pnp	Purine nucleoside phosphorylase	-3.2	RNA-binding
5331037		Glutamine transport ATP-binding protein	-2.7	nucleoside binding
5331621		Integrase	-7.7	DNA metabolic process
5331277		Putative transposase for IS1272	-3.9	DNA metabolic process
5331047		A/G-specific adenine glycosylase	-3.2	DNA metabolic process
Signal transduction				
5331402		Nitrite transport protein	-3.0	Two-component system

*Bolded gene IDs were related with dual-mechanism of erythorbyl laurate.

3-8. Validation of RNA-Seq data validation by qRT-PCR

The qRT-PCR was used to verify transcriptional profiling from RNA-Seq data. The randomly selected up-regulated genes related various categories of cell metabolism pathways and genes related with *vraSR* were subjected to qRT-PCR for validation of results from RNA-Seq.

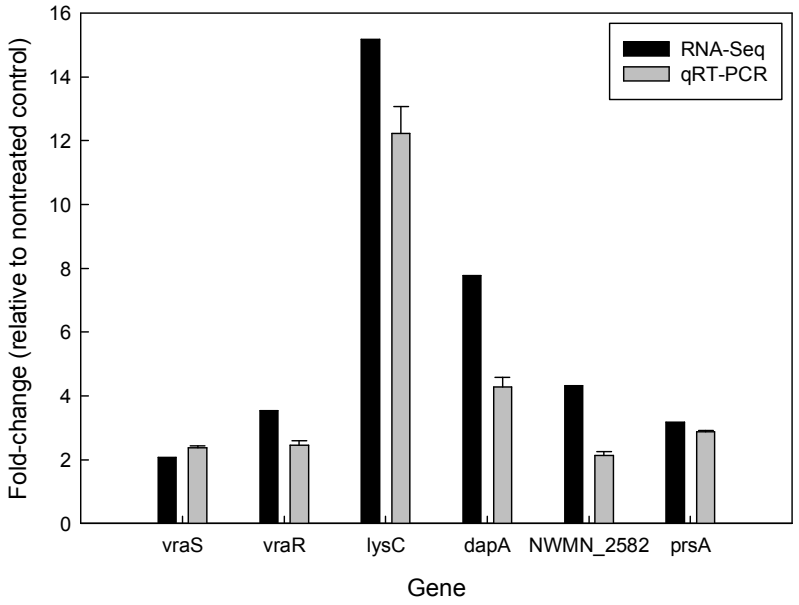

Fig. 10. qRT-PCR for validation of results from RNA-Seq.

4. Reference

Bechert, T., Steinrucke, P., & Guggenbichler, J. (2000). A new method for screening anti-infective biomaterials. *Nature Medicine, 6*(9), 1053-1056.

Bharali, P., Saikia, J., Ray, A., & Konwar, B. (2013). Rhamnolipid (RL) from Pseudomonas aeruginosa OBP1: A novel chemotaxis and antibacterial agent. *Colloids and Surfaces B-Biointerfaces, 103*, 502-509.

Devi, K., Nisha, S., Sakthivel, R., & Pandian, S. (2010). Eugenol (an essential oil of clove) acts as an antibacterial agent against Salmonella typhi by disrupting the cellular membrane. *Journal of Ethnopharmacology, 130*(1), 107-115.

Driessen, A. J., van den Hooven, H. W., Kuiper, W., Van de Camp, M., Sahl, H.-G., Konings, R. N., & Konings, W. N. (1995). Mechanistic studies of lantibiotic-induced permeabilization of phospholipid vesicles. *Biochemistry, 34*(5), 1606-1614.

Friedman, L., Alder, J., & Silverman, J. (2006). Genetic changes that correlate with reduced susceptibility to daptomycin in Staphylococcus aureus. *Antimicrobial agents and chemotherapy, 50*(6), 2137-2145.

Gutierrez, J., Barry-Ryan, C., & Bourke, P. (2008). The antimicrobial efficacy of plant essential oil combinations and interactions with food ingredients. *International journal of food microbiology, 124*(1), 91-97.

Jin, J., Li, Z., Wang, S., Wang, S., Huang, D., Li, Y., Ma, Y., Wang, J., Liu, F., Chen, X., Li, G., Wang, X., Wang, Z., & Zhao, G. (2012). Isolation

and characterization of ZZ1, a novel lytic phage that infects Acinetobacter baumannii clinical isolates. *Bmc Microbiology, 12*(156).

Kim, Y.-H., & Chung, H.-J. (2011). The effects of Korean propolis against foodborne pathogens and transmission electron microscopic examination. *New biotechnology, 28*(6), 713-718.

Kuroda, M., Kuroda, H., Oshima, T., Takeuchi, F., Mori, H., & Hiramatsu, K. (2003). Two-component system VraSR positively modulates the regulation of cell-wall biosynthesis pathway in Staphylococcus aureus. *Molecular microbiology, 49*(3), 807-821.

Lieberman, S., Enig, M. G., & Preuss, H. G. (2006). A review of monolaurin and lauric acid: natural virucidal and bactericidal agents. *Alternative & Complementary Therapies, 12*(6), 310-314.

Magalhaes, L., & Nitschke, M. (2013). Antimicrobial activity of rhamnolipids against Listeria monocytogenes and their synergistic interaction with nisin. *Food Control, 29*(1), 138-142.

Muthaiyan, A., Silverman, J., Jayaswal, R., & Wilkinson, B. (2008). Transcriptional profiling reveals that daptomycin induces the Staphylococcus aureus cell wall stress stimulon and genes responsive to membrane depolarization. *Antimicrobial agents and chemotherapy, 52*(3), 980-990.

Nobmann, P., Bourke, P., Dunne, J., & Henehan, G. (2010). In vitro antimicrobial activity and mechanism of action of novel carbohydrate fatty acid derivatives against Staphylococcus aureus and MRSA. *Journal of Applied Microbiology, 108*(6), 2152-2161.

Pan, S., Cheung, W., & Link, A. (2010). Engineered gene clusters for the

production of the antimicrobial peptide microcin J25. *Protein Expression and Purification, 71*(2), 200-206.

Park, K., Lee, D., Sung, H., Lee, J., & Chang, P. (2011). Lipase-catalysed synthesis of erythorbyl laurate in acetonitrile. *Food Chemistry, 129*(1), 59-63.

Pietiainen, M., Francois, P., Hyyrylainen, H., Tangomo, M., Sass, V., Sahl, H., Schrenzel, J., & Kontinen, V. (2009). Transcriptome analysis of the responses of Staphylococcus aureus to antimicrobial peptides and characterization of the roles of vraDE and vraSR in antimicrobial resistance. *Bmc Genomics, 10*(429).

Pridmore, A., Burch, D., & Lees, P. (2011). Determination of minimum inhibitory and minimum bactericidal concentrations of tiamulin against field isolates of *Actinobacillus pleuropneumoniae*. *Veterinary microbiology, 151*(3), 409-412.

Salvucci, E., Saavedra, L., & Sesma, F. (2007). Short peptides derived from the NH2-terminus of subclass IIa bacteriocin enterocin CRL35 show antimicrobial activity. *Journal of Antimicrobial Chemotherapy, 59*(6), 1102-1108.

Sands, J., Landin, P., Auperin, D., & Reinhardt, A. (1979). Enveloped virus inactivation by fatty-acid derivatives. *Antimicrobial agents and chemotherapy, 15*(1), 134-136.

Stocks, S. M. (2004). Mechanism and use of the commercially available viability stain, BacLight Cytometry Part A. *Cytometry Part A*, *61*(2), 189-195.

Utaida, S., Dunman, P., Macapagal, D., Murphy, E., Projan, S., Singh, V., Jayaswal, R., & Wilkinson, B. (2003). Genome-wide transcriptional

profiling of the response of Staphylococcus aureus to cell-wall-active antibiotics reveals a cell-wall-stress stimulon. *Microbiology, 149*(10), 2719-2732.

Wiegand, I., Hilpert, K., & Hancock, R. E. (2008). Agar and broth dilution methods to determine the minimal inhibitory concentration (MIC) of antimicrobial substances. *Nature protocols, 3*(2), 163-175.

Wilkinson, B. J., Muthaiyan, A., & Jayaswal, R. K. (2005). The cell wall stress stimulon of Staphylococcus aureus and other gram-positive bacteria. *Current Medicinal Chemistry-Anti-Infective Agents, 4*(3), 259-276.

국문초록

Erythorbic acid 는 L-ascorbic acid 의 이성질체로서 항산화제로 흔히 쓰이며, 상대적으로 L-ascorbic acid 에 비하여 경제적인 측면을 가지고 있다. 이러한 이유로 선행연구에서는 erythorbic acid 와 항균성을 가지는 중쇄 지방산인 lauric acid 를 기질로서 lipase 에 의한 esterification 을 통하여 erythorbyl laurate 를 합성하였고, 이로 인해 항산화성과 항균성을 동시에 지닌 유화제로 사용할 수 있게 되었다. 현재 erythorbyl laurate 의 기능성을 분석하여 이를 산업에 이용하고자 다양한 연구가 수행되고 있다. 본 연구는 erythorbyl laurate 의 항균성 메커니즘을 규명하고자 다양한 생리화학적 실험법과 전사 분석을 위한 RNA-Seq 기법을 이용하여 대표적인 유해 미생물 중 하나인 *Staphylococcus aureus* 에 대한 erythorbyl laurate 의 효과를 검증하였다. Erythorbyl laurate 는 그람 양성균에 특이적으로 효과를 보였고, 처리한 erythorbyl laurate 의 농도가 증가할수록 유도기(Δλ)는 증가하고 최대비성장률(μ_{max})은 감소하는 경향을 보였다. Crystal violet 과 SYTO 9, propidium iodide 를 이용한 실험에서는 erythorbyl laurate 에 의한 세포막 손상으로 인해 막 투과성이 변한다는 것을 확인하였다. 형광 현미경과 EF-TEM 을 이용하여 이에 대한 형태학적 분석을 수행한 결과, erythorbyl laurate 로 인해 세포 내 물질의 방출과

세포 표면의 손상 등의 물리적인 변화가 일어남을 관찰할 수 있었다. 또한 다양한 항균제와의 상승효과에 관해 연구한 결과, erythorbyl laurate 는 nisin, kanamycin, erythromycin 과 뛰어난 상승효과를 보였다. RNA-Seq 기법을 이용한 전사체 분석에서는 아미노산 합성, 단백질 기능, 세포막과 세포벽의 합성, 신호전달체계와 같은 다양한 세포 내 대사에 관여하는 유전자의 발현 차이를 관찰할 수 있었다. 이러한 결과를 바탕으로 erythorbyl laurate 가 세포벽에 자극을 주고 세포막의 손상을 일으키며, 이로 인해 균체의 다양한 대사체계가 영향을 받는다는 것을 알 수 있었다.

본 연구는 효소적 합성을 통해 생산된 erythorbyl laurate를 다기능성 식품첨가물로서 산업에 적용하기 위한 기초 연구로, erythorbyl laurate의 항균력을 검증하고 메커니즘을 밝힘으로써 식품뿐만 아니라 그람 양성균을 제어할 필요가 있는 다양한 분야에서 활용될 수 있는 가능성을 제시하는 것에 의의가 있다.